JID Open

Hyper-Inflammation and Skin Destruction Mediated by Rosiglitazone Activation of Macrophages in IL-6 Deficiency

Lopa M. Das[1], Julie Rosenjack[1], Liemin Au[1], Pia S. Galle[2,3], Morten B. Hansen[2], Martha K. Cathcart[4], Thomas S. McCormick[1], Kevin D. Cooper[1], Roy L. Silverstein[5] and Kurt Q. Lu[1]

Injury initiates recruitment of macrophages to support tissue repair; however, excessive macrophage activity may exacerbate tissue damage causing further destruction and subsequent delay in wound repair. Here we show that the peroxisome proliferation–activated receptor-γ agonist, rosiglitazone (Rosi), a medication recently reintroduced as a drug to treat diabetes and with known anti-inflammatory properties, paradoxically generates pro-inflammatory macrophages. This is observed in both IL-6-deficient mice and control wild-type mice experimentally induced to produce high titers of auto-antibodies against IL-6, mimicking IL-6 deficiency in human diseases. IL-6 deficiency when combined with Rosi-mediated upregulation of suppressor of cytokine signaling 3 leads to an altered ratio of nuclear signal transducer and activator of transcription 3/NF-κB that allows hyper-induction of inducible nitric oxide synthase (iNOS). Macrophages activated in this manner cause *de novo* tissue destruction, recapitulating human chronic wounds, and can be reversed *in vivo* by recombinant IL-6, blocking macrophage infiltration, or neutralizing iNOS. This study provides insight into an unanticipated paradoxical role of Rosi in mediating hyper-inflammatory macrophage activation significant for diseases associated with IL-6 deficiency.

Journal of Investigative Dermatology (2015) **135,** 389–399; doi:10.1038/jid.2014.375; published online 9 October 2014

INTRODUCTION

Suppressing inflammation often treats or prevents disease progression in numerous destructive, degenerative, and autoimmune conditions. Dysregulated inflammation may result in prolonged macrophage activation and aberrant production of pro-inflammatory cytokines resulting in damage to the surrounding tissue (Akiyama *et al.*, 2000; Pearson *et al.*, 2003; Fujiwara and Kobayashi, 2005; Hotchkiss and Nicholson, 2006). Rosiglitazone (Rosi), an insulin sensitizer, has recently been revived by the Food and Drug Administration to treat patients with type 2 diabetes mellitus, an indication similar to other diabetes drugs currently available. Rosi belongs to the thiazolidinedione class of drugs, which are ligands for the nuclear hormone receptor peroxisome proliferation–activated receptor-γ (PPAR-γ), and have been shown to attenuate inflammation in experimental injury models (Park *et al.*, 2003; Cuzzocrea *et al.*, 2004; Hasegawa-Moriyama *et al.*, 2012). Mechanistically, Rosi action on macrophages enhances tissue repair by decreasing tumor necrosis factor (TNF)-α and inducible nitric oxide synthase (iNOS) via induction of suppressor of cytokine signaling (SOCS3), a negative regulator of signal transducer and activator of transcription 3 (STAT3)-dependent cytokine signaling (Jiang *et al.*, 1998; Cuzzocrea *et al.*, 2004; Odegaard *et al.*, 2007; Sener *et al.*, 2007; Chatterjee, 2010). SOCS3 expression is regulated by IL-6, a pleiotropic acute-phase mediator with dual pro- and anti-inflammatory effects (Xing *et al.*, 1998; Li *et al.*, 2012; Tanaka and Kishimoto, 2012). Recently, we demonstrated increased prevalence of impaired IL-6 signaling in people with type 2 diabetes, as a result of IL-6 deficiency mediated by development of auto-antibodies to IL-6 (aAB-IL6; Fosgerau *et al.*, 2010; Awazawa *et al.*, 2011). We have shown that generation of human-equivalent titers of aAB-IL-6 in mice leads to impaired IL-6 signaling and impaired glucose tolerance (Ciapponi *et al.*, 1997; Galle *et al.*, 2004; Puel *et al.*, 2008). As the primary indication of Rosi is in type-2 diabetics, we wanted to examine its anti-inflammatory effects in the setting of impaired IL-6 signaling.

[1]*Department of Dermatology, Case Western Reserve University, Cleveland, Ohio, USA;* [2]*Centre of Inflammation and Metabolism, Rigshospitalet, National University Hospital, Copenhagen, Denmark;* [3]*Department of Clinical Immunology, Rigshospitalet, National University Hospital, Copenhagen, Denmark;* [4]*Department of Cellular and Molecular Medicine, Lerner Research Institute, Cleveland Clinic Foundation, Cleveland, Ohio, USA and* [5]*Department of Medicine, Medical College of Wisconsin, Milwaukee, Wisconsin, USA*

Correspondence: Kurt Q. Lu, Department of Dermatology, Case Western Reserve University, 2109 Adelbert Road, BRB 529, Cleveland, Ohio 44106, USA. E-mail: kurt.lu@case.edu

Abbreviations: aABIL-6, auto-antibodies to IL-6; iNOS, inducible nitric oxide synthase; LPS, lipopolysaccharide; NF-κB, nuclear factor kappa B; ODN, oligodeoxyribonucleotide; PBS, phosphate-buffered saline; PPAR-γ, peroxisome proliferation–activated receptor gamma; pSTAT3, phosphorylated signal transducer and activator of transcription 3; Rosi, rosiglitazone; SOCS3, suppressor of cytokine signaling; TNF, tumor necrosis factor

Received 5 November 2013; revised 22 May 2014; accepted 28 May 2014; accepted article preview online 3 September 2014; published online 9 October 2014

Our data show the effect of Rosi combined with IL-6 deficiency *in vitro* and *in vivo* results in generation of pro-inflammatory iNOS-expressing macrophages via a SOCS3-mediated altered nuclear STAT3/NF-κB ratio. Treatment with Rosi of wild-type (WT) mice possessing high levels of aAB-IL-6 and IL-6$^{-/-}$ mice resulted in drastic macrophage-mediated *de novo* tissue destruction and delayed wound healing. The data highlight a pivotal role of IL-6 deficiency in Rosi-mediated activation and polarization of macrophages in an experimental model system. Given the common co-occurrence of autoantibody-mediated IL-6 deficiency and usage of thiazolidinedione medications, these findings may provide insight into recent negative outcomes in subsets of diabetics.

RESULTS

Macrophage infiltration at the site of injury leads to tissue destruction and delayed wound healing

We investigated the immune-modulatory effects of topical Rosi on wound healing in IL-6$^{-/-}$ mice using a skin injury model. The use of a one-time low-dose UV exposure to a clean surgical excision allows for exacerbation of inflammation through infiltration of activated macrophages to the excision site. UV used in this model of inflammatory wounds allows for accuracy in delivering a calibrated dose, thereby minimizing inter-experimental variability. IL-6$^{-/-}$ mice subjected to the wound protocol demonstrate visible erythema in regions between open wounds with little contraction compared with WT. By day 9, WT mice progressed toward resolution. In IL-6$^{-/-}$ mice, however, the wounds remained enlarged above baseline, ultimately requiring 23 days for complete resolution (Figure 1a and b). When IL-6$^{-/-}$ mice were administered recombinant IL-6, the mice displayed wound healing with resolution comparable to WT, validating the critical role of IL-6 in this phenotype (Figure 1b). Rosi induced an inflammatory response only in IL-6$^{-/-}$ mice subject to the inflammatory wound model and not in IL-6$^{-/-}$ or WT mice with surgical excision alone (no UVB; Supplementary Figure 1a–d online).

Concurrent with delayed wound healing in IL-6$^{-/-}$ mice subjected to the wound protocol, we show histologically that 24 hours post treatment with Rosi, there is disruption of skin architecture with epidermal erosion and underlying tissue destruction that extended beyond the dermis (Figure 1c isotype control). As the immediate effect of skin injury is marked by a massive infiltration of mononuclear cells especially macrophages, we tested whether inhibiting macrophage entry into the skin restores tissue morphology. Blocking with anti-CD11b antibody *in vivo* has been previously shown to prevent infiltration of monocytic cells into the skin (Hammerberg *et al.*, 1996; Qi *et al.*, 2008). In our model, anti-CD11b-treated IL-6$^{-/-}$ mice demonstrated intact epidermis and dermis with a sparse mononuclear infiltrate in the subcutis (Figure 1c panel 2) compared with isotype control (Figure 1c panel 3), which displayed epidermal necrosis, superficial dermal necrosis, dermal edema, and a dense infiltrate of inflammatory cells in the subcutis. Confocal microscopy confirmed decreased macrophages (CD11b^{+}/F4/80^{+} cells) in the skin of anti-CD11b-treated mice both in the dermis and the subcutis (Figure 1d dermis panel 2, subcutaneous panel 2) and demonstrated accelerated wound healing and full closure by day 13 (Figure 1e).

To determine whether infiltrating monocytes are responsible for the excess inflammation, we injected the skin of IL-6$^{-/-}$ mice with clodronate liposomes, a drug toxic to phagocytic cells upon engulfment of the liposome. After 24 hours, the skin at the wound edge from treated IL-6$^{-/-}$ mice had normal appearing epithelia with preservation of the epidermis and dermis and sparse mononuclear cell infiltrates in the dermis and subcutis (Figure 1f). In contrast, treatment with control phosphate-buffered saline (PBS)-filled liposomes exhibited dermal edema, epidermal necrosis, and superficial dermal necrosis (Figure 1g). By 48 hours, the edema became massive, whereas a drastic reduction in mononuclear cells was observed in clodronate liposome–treated skin (Figure 1f panel 2 vs. Figure 1g panel 2). On the basis of skin histology and the ability of clodronate to accelerate wound healing, we demonstrate that treatment with Rosi in this inflammatory wound mouse model drives macrophage entry into the wound to modulate inflammation and tissue destruction.

Hyper-inflammatory macrophages exacerbate iNOS-mediated inflammation and delay wound healing at the site of injury

Activation of iNOS is well established in models of macrophage-mediated inflammation, and our data show that treatment with Rosi of IL-6$^{-/-}$ mice resulted in inflammation associated with marked increase in iNOS mRNA levels from the skin around the wounds at 12 hours that sustained for 24 hours (Figure 2a). No upregulation was observed in WT mice. In both WT and IL-6$^{-/-}$ mice, inflammatory infiltrates were observed in histological sections mainly in the deeper dermis and subcutis in the skin around the wounds (Figure 2b panel 1, Figure 2c panel 1). Confocal microscopy of serial sections shows that WT animals had low levels of iNOS (Figure 2b panel 1) with macrophages staining CD11b^{+}F4/80^{+} but faintly for iNOS (indicated with white arrows), whereas IL-6$^{-/-}$ mice with same treatment condition show robust staining for iNOS colocalizing with CD11b^{+}F4/80^{+} (marked with white arrows; Figure 2c panel 2). To determine a role for iNOS in mediating delayed healing, IL-6$^{-/-}$ mice treated with the compound 1,400 W, a specific iNOS inhibitor before wounding protocol, restored healing to 14 days (Figure 2d), suggesting a role for iNOS. Mice subjected to wound protocol were also given an i.p. injection of PBS as vehicle control. In parallel studies, IL-6$^{-/-}$ mice injected with anti-TNF-α showed accelerated wound healing compared with isotype-treated control mice (Supplementary Figure 2 online). Thus, IL-6 deficiency and Rosi treatment of mice drive macrophage infiltration and activation (high iNOS and TNF-α) toward a hyper-inflammatory state, propagating inflammation and tissue destruction.

Mechanism of Rosi-mediated elevation of iNOS in macrophages in the absence of IL-6

To appreciate a direct effect of Rosi on iNOS production *in vitro,* IL-6$^{-/-}$ and WT thioglycollate-elicited peritoneal macrophages were dosed with Rosi. Treatment of IL-6$^{-/-}$

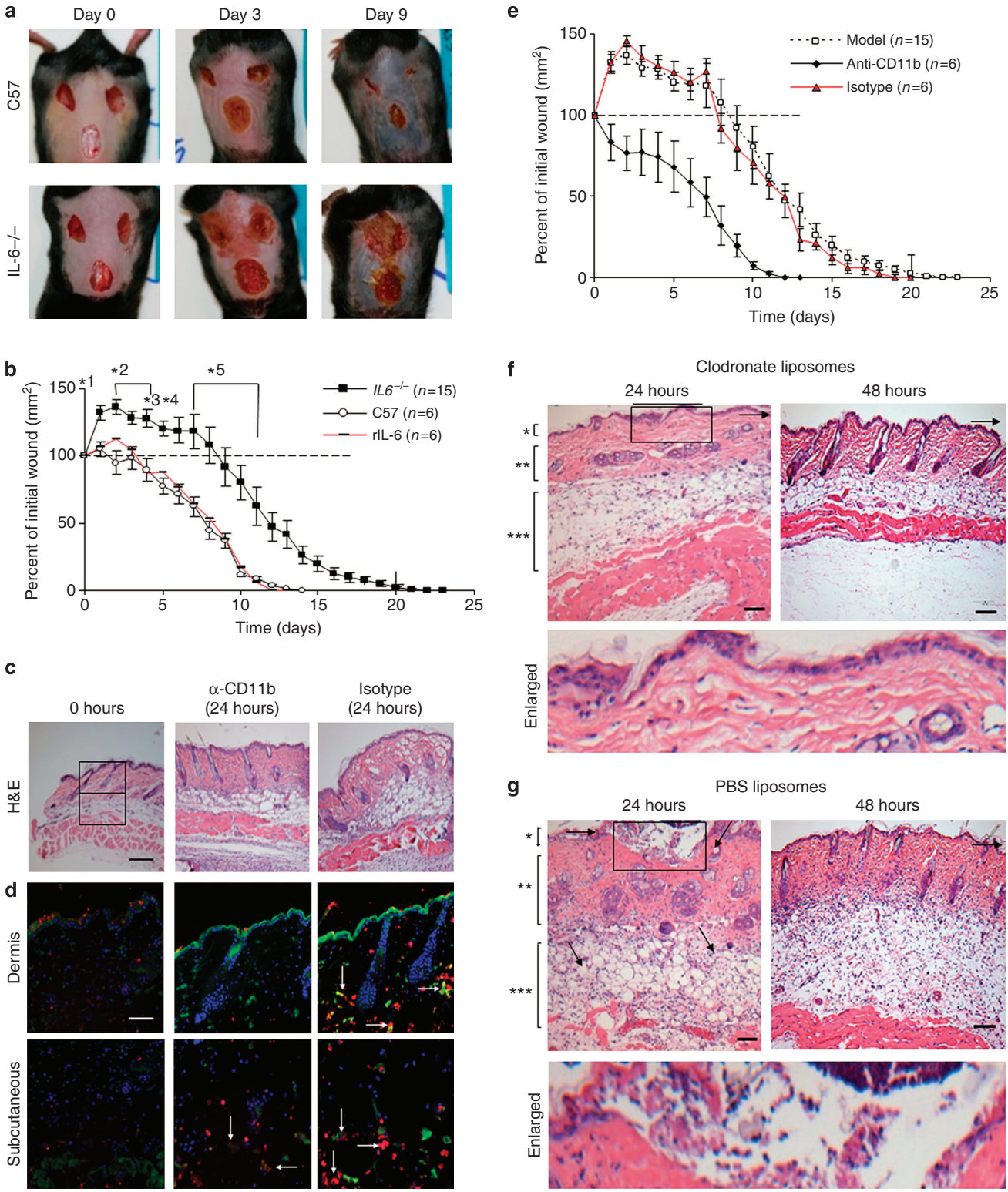

Figure 1. Macrophage infiltration is necessary for delayed wound healing and tissue destruction. Wild-type and IL-6$^{-/-}$ mice, subjected to wounding protocol, are depicted (**a**) in images and (**b**) graphically (*1P<0.01, *2P<0.005, *3P<0.001, *4P<0.01, and *5P<0.05). Dotted line indicates ''baseline'' percentage of wound area. Wound healing in the presence or absence of CD11b blocking antibody or isotype is shown by (**c**) hematoxylin and eosin (H&E) staining (bar = 100 μm), (**d**) confocal images of immunostaining for F4/80 (green), CD11b (red), and nucleus (blue), and (**e**) graphically. Wounds from IL-6$^{-/-}$ mice were injected intradermally with (**f**) clodronate liposomes and (**g**) control phosphate-buffered saline (PBS)-liposomes at 24 and 48 hours. Epidermal necrosis (*), superficial dermal necrosis, dermal edema (**), and inflammatory cells in the subcutis (***) indicated. Box—epidermal–dermal junction. Arrow—wound edge. Bar = 40 μm.

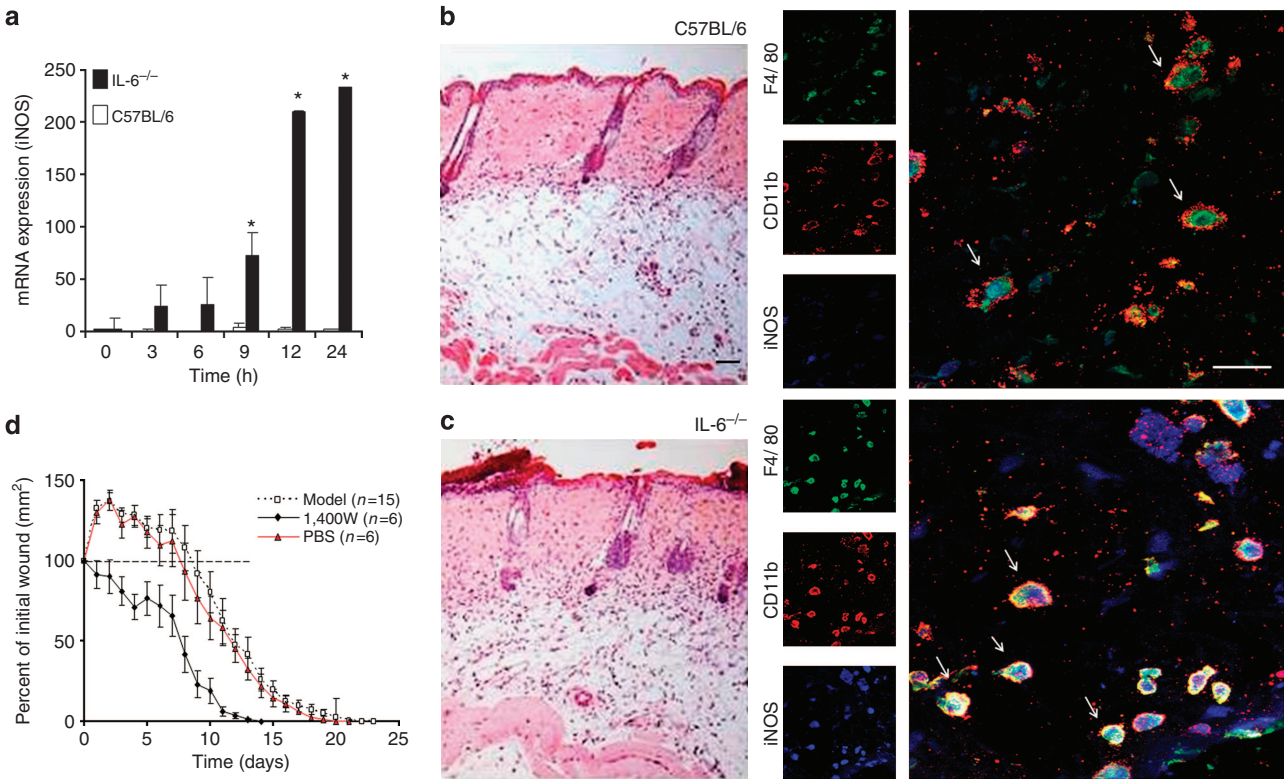

Figure 2. Activation of infiltrated macrophages in the skin results in tissue destruction and delayed wound healing. (**a**) Quantification of inducible nitric oxide synthase (iNOS) mRNA expression from the skin surrounding the wound edge of IL-6$^{-/-}$ and control C57BL6 mice at indicated time points post rosiglitazone (Rosi) treatment. Values are means ± SE. *P<0.01, n=3 mice. Hematoxylin and eosin stains of histological sections in (**b**) control and (**c**) IL-6$^{-/-}$ skin. Confocal images of skin sections from (**b**) C57BL6 mice and (**c**) IL-6$^{-/-}$ mice after immunostaining for iNOS (blue) and CD11b^{+} (red) and F4/80^{+} (green) cells. Bar = 40 μm. (**b**, **c**) Arrows indicate co-localization of iNOS with macrophages in C57BL/6 and *IL6*$^{-/-}$ section. (**d**) The wound healing capacity was measured in Rosi-treated IL-6$^{-/-}$ mice in the presence or absence of iNOS-specific inhibitor, 1,400 W. PBS, phosphate-buffered saline.

lipopolysaccharide (LPS)–primed macrophages caused marked induction of iNOS mRNA compared with that in WT, which remained at baseline (Supplementary Figure 3 online), suggesting that Rosi treatment of macrophages initiates an intracellular signaling cascade to promote transcription of *Nos2*. However, using MAPPER that applies the recommended stringencies of low *E*-values (<0.1) and high scores (>5), analysis of *Nos2* showed no PPAR-γ response elements in the promoter region of the gene (Marinescu *et al.*, 2005). In addition, there is no direct link between PPAR-γ and the major transcription factor for iNOS, NF-κB (Ingenuity Pathways; Pahan *et al.*, 2001; Lawrence, 2009) reflecting potential receptor-independent effects of Rosi on inflammation. As PPAR-γ ligands have been shown to induce SOCS3, we hypothesized that SOCS3 has an indirect role in regulating NF-κB activity in our wound model. Cytoplasmic SOCS3 inhibits phosphorylation of STAT3 and its subsequent nuclear translocation (Qin *et al.*, 2012). Nuclear STAT3 transrepresses NF-κB, resulting in decreased iNOS expression (Yu *et al.*, 2002; Yu and Kone, 2004). We observed basal levels of cytoplasmic SOCS3, reflective of a relative state of activation resulting from thioglycollate elicitation of WT macrophages (Figure 3a). SOCS3 was robustly increased in IL-6$^{-/-}$ macrophages pretreated (16 hours) with Rosi *in vitro* followed by LPS stimulation (15 minutes; Figure 3a lane 4). LPS priming of IL-6$^{-/-}$ and WT macrophages modestly increased cytoplasmic phosphorylated STAT3 (pSTAT3) at 30 minutes (Figure 3b lane 3). In contrast, Rosi pretreatment of IL-6$^{-/-}$ LPS–primed macrophages resulted in almost complete loss of cytoplasmic pSTAT3 (correlating with high levels of SOCS3; Figure 3b lane 5). Supplementation with recombinant IL-6 robustly restored pSTAT3 in IL-6$^{-/-}$ macrophages (Figure 3b lane 6).

Next, we determined whether Rosi-mediated decrease in cytoplasmic pSTAT3 alters nuclear STAT3. In contrast to WT macrophages treated with Rosi and LPS, IL-6$^{-/-}$ macrophages had undetectable nuclear STAT3. These cells concomitantly had robust increases in nuclear NF-κB (Figure 3c, lane 4). Supplementation with recombinant IL-6 restored nuclear STAT3 in IL-6$^{-/-}$ macrophages, resulting in an NF-κB/STAT3 profile and ratio similar to WT macrophages (Figure 3b lane 5, 3c lane 5). In summary, the IL-6-deficient condition where pronounced iNOS hyper-induction is observed is one in which cytoplasmic SOCS3 is increased, cytoplasmic-pSTAT3 is decreased, and nuclear STAT3 is absent, resulting in a skewing of nuclear NF-κB/STAT3 ratios (Figure 3a–d), thus defining the downstream biochemical steps following Rosi treatment in WT versus *IL6*−/−-activated macrophages *in vitro*.

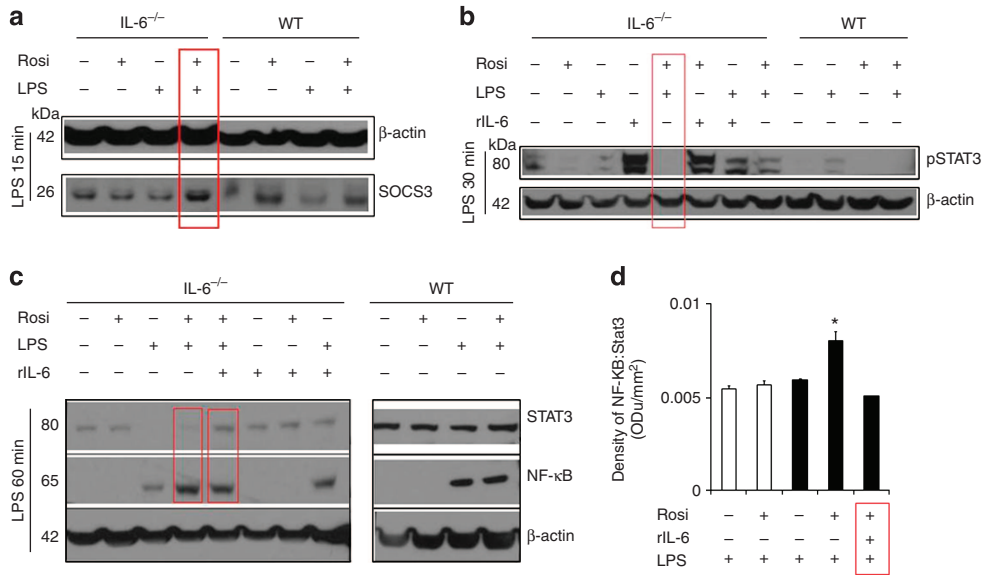

Figure 3. Increased suppressor of cytokine signaling 3 (SOCS3) regulates NF-κB-induction of inducible nitric oxide synthase (iNOS) in IL-6-deficient macrophages. Peritoneal macrophages from IL-6$^{-/-}$ and wild-type (WT) mice were pretreated with rosiglitazone (Rosi) for 16 hours and stimulated with lipopolysaccharide (LPS) to detect (**a**) cytoplasmic SOCS3, (**b**) phospho-signal transducer and activator of transcription 3 (STAT3; $n=3$ mice), (**c**) nuclear localization of NF-κBp65 and STAT3 ($n=3$ mice), and (**d**) the ratio of NF-κBp65 to STAT3 ($n=3$, $^{*}P=0.0021$) with and without recombinant IL-6 (rIL-6). Open bar graphs represent WT, and filled bars represent IL-6$^{-/-}$ macrophages.

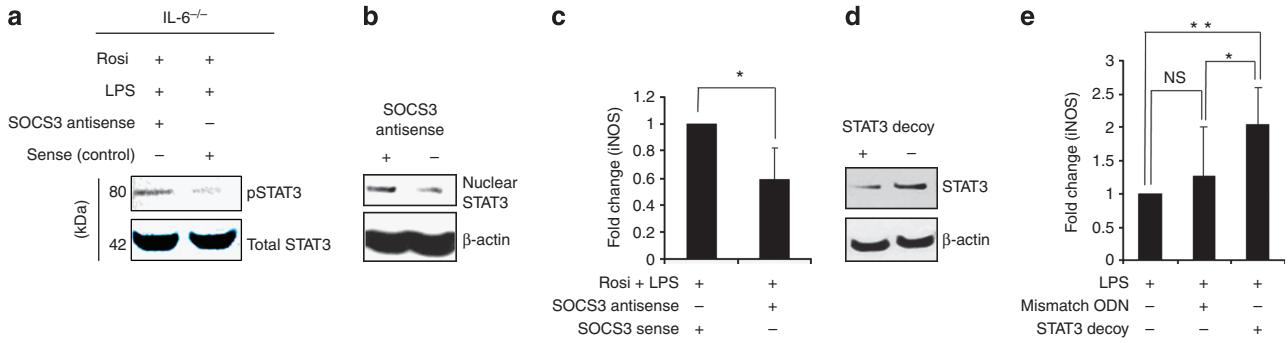

Figure 4. Removal of suppressor of cytokine signaling 3 (SOCS3) allows nuclear translocation of signal transducer and activator of transcription 3 (STAT3) and promotes inducible nitric oxide synthase expression in the absence of IL-6. Pretreated IL6$^{-/-}$ bone marrow–derived macrophages (BMDMs) transfected with SOCS3 antisense oligonucleotides were stimulated with lipopolysaccharide (LPS); (**a**) to detect cytoplasmic phospho-STAT3, (**b**) to measure nuclear translocation of STAT3, and (**c**) to assess inducible nitric oxide synthase (iNOS) mRNA expression at 4 hours. Values are means ± SE. $^{*}P=0.017$, ($n=5$ mice). To demonstrate iNOS dependence of STAT3 (**d**) IL6$^{-/-}$ BMDMs were also treated with the STAT3 decoy and (**e**) stimulated with LPS for 4 hours for detection of iNOS mRNA. $n=5$ mice, $^{*}P=0.04$, $^{**}P=0.0148$. NS, not significant; ODN, oligodeoxyribonucleotide.

As hyper-induction of iNOS was seen only in IL-6$^{-/-}$ macrophages, we next determined whether inhibition of SOCS3 in these cells before Rosi and LPS treatment would decrease iNOS expression. Transfection of bone marrow–derived macrophages with a SOCS3-specific antisense oligodeoxyribonucleotide (ODN) resulted in transient knockdown of SOCS3 (Supplementary Figure 4 online), restored cytoplasmic pSTAT3 expression at 30 minutes (Figure 4a), nuclear STAT3 (Figure 4b) culminating in a 59% decrease in iNOS expression (Figure 4c). The observations strengthen our findings that Rosi treatment of macrophages sets off SOCS3 induction of iNOS by STAT3 in an IL6^{-}-dependent manner. Therefore, targeting STAT3 without Rosi should recapitulate the effect mediated by Rosi treatment. IL-6$^{-/-}$ macrophages were transfected with a STAT3-consensus-binding-sequence (STAT3 decoy). Independent of Rosi activation of macrophages, STAT3 decoy decreased nuclear STAT3 (Figure 4d), resulting in a 2.4-fold increase in iNOS mRNA (Figure 4e). Sense ODN served as control. Statistical comparisons demonstrate that interfering specifically with STAT3 significantly elevated iNOS compared with LPS alone or the ODN control. Collectively, the *in vitro* data demonstrate that, in an inflammatory response, Rosi treatment in IL-6 deficiency initiates the PPAR-γ-SOCS3-STAT3 signaling cascade that modulates the expression of NF-κB and ultimately drives iNOS expression.

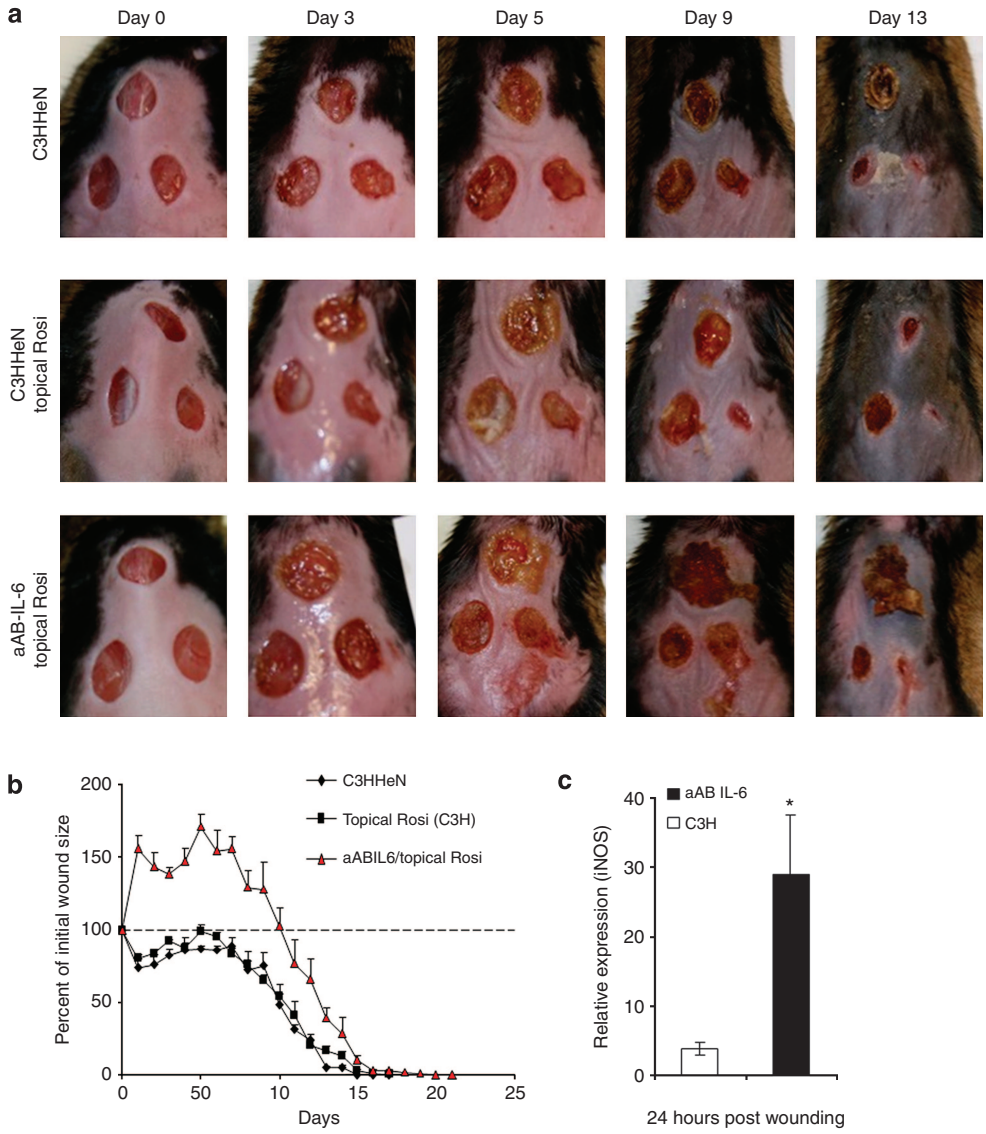

Figure 5. Rosiglitazone (Rosi) treatment in the presence of auto-antibodies against IL-6 drives increased inducible nitric oxide synthase (iNOS) expression and delayed wound healing. Female C3HHeN mice were immunized with IL-6 analogs to induce aABIL-6 before experimentation. Age-matched C3HHeN mice with topical Rosi in the presence or absence of circulating aAB-IL-6 were subjected to the wounding protocol. (**a**) The exacerbation of wound formation and the rate of wound healing was monitored, (**b**) wound healing was quantitated as a percent of initial wound size $n=3$ mice, and (**c**) RNA was extracted from the skin of all three experimental groups at 24 hours post aABIL-6 treatment for analysis of iNOS mRNA expression. Values are means ± SE. $^*P<0.05$, $n=4$.

Rosi drives hyper-inflammation and tissue destruction in autoantibody-mediated deficiency of IL-6

Next, we sought to determine the effect of Rosi in states of physiologic IL-6 deficiency. We previously demonstrated that aAB-IL-6 is measurable in 10% of Danish blood donors with 0.1% of them producing high amounts of neutralizing aAB-IL-6 (Hansen *et al.*, 1991; Galle *et al.*, 2004; Fosgerau *et al.*, 2010). To determine whether *in vivo* autoantibody-mediated deficiency of IL-6 combined with Rosi would drive hyper-inflammation and tissue destruction, we used a vaccination protocol based on murine IL-6 analogs that induces high titers of aAB-IL-6 (Ciapponi *et al.*, 1997; Galle *et al.*, 2007). Control (C3HEN) and aAB-IL-6 mice were then subjected to the previously described inflammatory wound protocol with topical Rosi. By day 3, wounds in aAB-IL-6 mice were enlarged with little contraction compared with controls. By day 9, the wounds of C3HEN mice had progressed toward resolution, whereas the wounds of the aAB-IL-6 mice remained enlarged (Figure 5a and b). Strikingly, wound closure was delayed by 5 days in these mice compared with controls (Figure 5b). At 24 hours, wound areas of aAB-IL-6 mice were 50% larger compared with initial wound size (Figure 5a and b), which corresponded to a significant increase in iNOS relative mRNA expression (Figure 5c) from skin biopsies obtained from the wound. Thus, iNOS induction of aAB-IL-6-induced mice is reminiscent of high iNOS levels in IL-$6^{-/-}$ mice subject to our treatment protocol (Figure 2a) and supports our hypothesis that the observed paradoxical

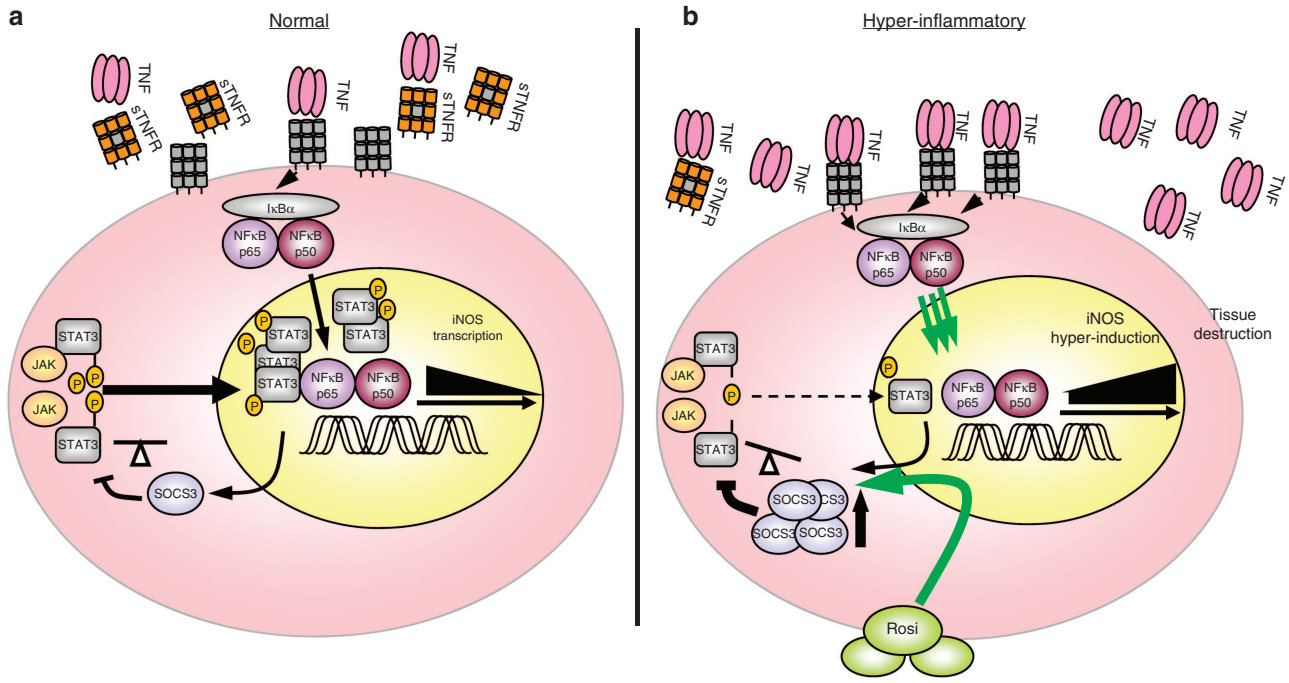

Figure 6. Model of mechanisms modulating inflammatory responses. (**a**) Following stimulation, macrophages release soluble tumor necrosis factor (TNF)-α receptor (sTNFR) to dampen the effects of TNF-α, whereas activation of signal transducer and activator of transcription 3 (STAT3) acts to repress NF-κB activity, resulting in regulated inducible nitric oxide synthase (iNOS) expression. (**b**) In the absence of IL-6, sTNFR release is diminished, allowing for increased NF-κB activity. Concurrently, rosiglitazone (Rosi) treatment results in upregulation of suppressor of cytokine signaling 3 (SOCS3) that decreases STAT3 activation. This prevents nuclear translocation of activated STAT3 resulting in loss of NF-κB transrepression. The net result of decreased NF-κB transrepression and simultaneous increased NF-κB activity via TNF-α and other pro-inflammatory cytokines drives increased iNOS expression and subsequent tissue damage.

hyper-inflammatory effect of Rosi is due to a deficiency in IL-6 and its signaling.

DISCUSSION

The thiazolidinedione class of drugs have previously been shown to be anti-inflammatory and capable of generating alternatively activated macrophages that function to attenuate inflammatory mediators like iNOS and COX2 (Jiang *et al.*, 1998; Ricote *et al.*, 1998; Feinstein *et al.*, 2005; Hasegawa-Moriyama *et al.*, 2012); however, our data show a deviation from the anti-inflammatory response to this medication. We demonstrate that the net response of Rosi treatment and concomitant IL-6 deficiency is a paradoxical exacerbation of inflammation. Rosi in this capacity may be acting through the PPAR-γ receptor but may also have receptor-independent effects. Direct evidence for PPAR-γ-independent effects comes from studies in which PPAR-γ antagonists were unable to block anti-inflammatory actions in LPS-stimulated cells, and PPAR-γ deficiency did not affect Rosi (and pioglitazone)-mediated production of prostaglandin (Tsukamoto *et al.*, 2004; Feinstein *et al.*, 2005). Moreover, Rosi inhibited iNOS function in activated macrophages at a concentration 650-fold higher than its EC-50 value for binding PPAR-γ, indicative of multiple effects of Rosi on the cell beyond receptor-mediated signaling (Ricote *et al.*, 1998). Our data show that Rosi increases SOCS3, transiently altering the nuclear STAT3/NF-κB ratio by decreasing STAT3 translocation into the nucleus. Decreased nuclear accumulation of STAT3 regulates the expression of NF-κB-responsive genes such as iNOS, via reduced transrepression of NF-κB (Figure 6a and b; Yu *et al.*, 2002; Park *et al.*, 2003; Yu and Kone, 2004).

Hyper-inflammation is attenuated by endogenous inhibitors of pro-inflammatory cytokines such as soluble TNF-α receptor that helps regulate and limit inflammatory signals (Tilg *et al.*, 1994; Sikora *et al.*, 2008, 2009). Concurrent with other studies (Tilg *et al.*, 1994), examination of peritoneal fluid of thioglycollate-activated aAB-IL-6 mice showed significantly less secretion of soluble TNF-α receptor (Supplementary Figure 5 online). Thus, a limited capacity to downregulate extracellular cytokine stimulation in IL-6 deficiency combined with decreased NF-κB transrepression via Rosi results in hyper-inflammation. As SOCS3 and STAT3 form a regulatory feedback loop, these alterations represent a transient escape from regulated inflammatory responses resulting in hyper-inflammation. The parallels of both the *in vivo* and *in vitro* studies demonstrate that indeed Rosi and IL-6 deficiency together show paradoxical hyper-activation of macrophage. Taken together, the model of delayed wound healing proposed requires Rosi/SOCS3 induction of iNOS via increased NF-κB activation coupled to decreased transrepression of NF-κB culminating in excessive inflammation and tissue destruction (Figure 6a and b). Although we tested the contribution of hyper-activated macrophages that prolong inflammation and delay wound healing in our Rosi study model, our findings may be relevant to other cell types that populate the wound

bed after tissue injury. Infiltrating neutrophils are a source of iNOS that may contribute to damage of surrounding tissue (Tsukahara *et al.*, 2001). In this model, we speculate that neutrophils enhance the chemoattraction for macrophages into the wound bed but are not the critical cellular source of iNOS at later stages of the tissue destruction. Subsets of dendritic cells, specifically plasmacytoid dendritic cells, have an important role in wound healing. In response to nucleic acids from cellular debris, plasmacytoid dendritic cells secrete type-1 IFNs to accelerate wound healing through reepithelialization of injured skin (Gregorio *et al.*, 2010). As DC function is affected by PPAR-γ ligands (Faveeuw *et al.*, 2000; Hammad *et al.*, 2004), it is unclear in the IL-6-deficient system whether there is diminished type-1 IFN production, thereby indirectly contributing to delayed wound repair. In our IL-6-deficient skin injury model, treatment with Rosi may set off a similar influx of immune cells populating the wound, but the accumulation and activation of iNOS-producing macrophages may outnumber other cell types and impart a lasting and profound effect on the progression of inflammation.

These findings may be germane to wound healing and destructive inflammation in other organ systems. In addition, it will be of interest to determine whether a patient population showing auto-anti-IL6 antibodies will demonstrate elevated levels of iNOS in inflamed tissue. As there are other iNOS-responsive cells (Curran *et al.*, 1989; Campanholle *et al.*, 2010; Harbrecht *et al.*, 2012; Lowry *et al.*, 2013; Mao *et al.*, 2013; Wheeler *et al.*, 2013), this mechanism of hyper-induction of inflammation may be a common physiological response in mediating tissue destruction in other organs. The association of a paradoxical hyper-inflammatory state with Rosi and IL-6 deficiency provides insight into the cellular basis for clinical situations of non-resolving or exacerbated inflammation. aAB-IL-6 occurs naturally in 2–10% of the European and Japanese general population (Hansen *et al.*, 1991; Takemura *et al.*, 1992; Galle *et al.*, 2004), which increases with age, and recently shown to be more common in patients with rheumatic disease and type 2 diabetes (Fosgerau *et al.*, 2010). The combination of an injurious event in an aAB-IL-6 patient taking Rosi medication may result in hyper-inflammation. Therefore, screening for aAB-IL-6 in humans may have predictive value for preventing potential adverse effects of thiazolidinedione treatment therapies. In addition, the clinical scenario in which Rosi treatment coincides with IL-6 deficiency is not limited to prescribed medications as activation of PPAR-γ can result from many endogenous ligands such as oxidized lipids (Chomarat *et al.*, 2000; Liu *et al.*, 2012; Nagy *et al.*, 1998). With the widespread use of thiazolidinedione drugs prescribed for diabetes, several reports of unexplained increased edema and also increased fatal cardiac events with Rosi in diabetics (Rosen, 2007) raise the suspicion of hyper-inflammatory responses as a factor in these adverse outcomes. Furthermore, activated macrophages and exacerbated inflammation are known to contribute to the cardiovascular disease pathogenesis (Hansson, 2005). In conclusion, research designed to target hyper-inflammatory macrophages will likely improve the ability to treat chronic wounds and allow for development of a previously unreported therapeutic approach to other chronic conditions.

MATERIALS AND METHODS

Mice

Pathogen-free, 6- to 8-week-old female WT and IL-6$^{-/-}$ C57BL/6J mice were obtained from Jackson Laboratories (Bar Harbor, ME). Three- to four-week-old female C3HHeN mice were obtained from Harlan Industries. The animal studies have been approved by the Institutional Animal Care and Use Committee at Case Western Reserve University.

Immunofluorescence

Macrophages were defined as cells that stained positive for F4/80 and CD11b. For immunofluorescence staining of skin, 8 μm sections of frozen tissue were sectioned and fixed in 4 °C 100% acetone for 10 minutes. For immunofluorescence of lung tissue, 5 μm sections were fixed in formalin, embedded in paraffin, and deparaffinized in xylene and ethanol. Primary and secondary antibodies were diluted as indicated in 1 × PBS: anti-mouse F4/80 Antigen Alexa-488 BM8 (eBioscience, San Diego, CA, 1:100); rat monoclonal (M1/70) to CD11b APC/Cy7 (Abcam, Cambridge, MA, 1:20); and rabbit anti-iNOS/iNOS II, NT (Millipore, Billerica, MA, 1:50).

Reverse transcriptase–PCR

For reverse transcriptase–PCR analysis, RNA was isolated using Trizol (Invitrogen, Carlsbad, CA), following the manufacturer's instructions, and was reverse-transcribed and quantified using the Applied Biosystems TaqMan RNA-to-C_T 1-Step Kit, TaqMan Gene Expression Assays for 18s RNA, iNOS, TNF-α, and the Step-One System. Cycle time, temperature, and number were based on Applied Biosystems (Grand Island, NY) recommendations.

Wound preparation, treatment, and measurement

The skin was wounded as described. After shaving and chemical depilation of hair from the dorsal back skin, mice were allowed to rest for 48 hours. Using a template to mark out three circles of 6 mm diameter spaced apart in an equilateral triangle on dorsal skin, mice were subject to three excisional biopsies. Three wounds were chosen to capture variations in innate healing rates in each individual animal. To exacerbate inflammation in these clean surgical excisions, we exposed the wounds to a one-time single low dose of 72 mJ cm^{-2} UVB, a dose previously shown to enhance infiltration of monocytes and macrophages into the skin without inciting further injury (Baadsgaard *et al.*, 1987; Meunier *et al.*, 1995). At day 0, wounds were measured lengthwise and widthwise, exposed to 1 minimal erythema dose UVB, and treated topically with a 1% solution of Rosi in 10 g Aquaphor (Beiersdorf, Wilton, CT). Wounds were measured and topical Rosi solution applied daily until healed (loss of serum crust and reepithelialization).

Peritoneal macrophages

Mice were injected i.p. with 2 ml of thioglycollate and killed 24 hours later by cervical dislocation. Lavage was performed by infusing 5 ml of 4 °C Dulbecco's phosphate buffered saline into the peritoneal cavity. The fluid sample is recovered by aspirating the liquid with a syringe. A volume of 80% ± 21% of instilled fluid is recovered.

Bone marrow–derived macrophages

Briefly, bone marrow cells were flushed aseptically with PBS from the dissected femurs of mice. The cells were cultured on 25 cm^2 plates in DMEM containing 15% fetal calf serum, 1% penicillin/streptomycin, 1% L-glutamine, 4.5 $g\,l^{-1}$ glucose, and 20 $\mu g\,l^{-1}$ macrophage colony stimulating factor. After 6 days, media were changed to remove any cellular debris and non-adherent cells. The following day (day 7), the cells were carefully removed using lidocaine (4 $mg\,ml^{-1}$) and 10 mM EDTA in PBS at pH 7.5 and dispensed into six-well plates at a concentration of 2×10^6 cells per well. Before experimentation, media were replaced with macrophage colony stimulating factor-free media containing 5 mM L-arginine.

Western blot

The NE-PER kit (Thermo Scientific, Waltham, MA) was used to extract nuclear and cytoplasmic protein from peritoneal macrophages. Protein samples were prepared under reducing conditions, and western blot analysis was performed using a standard protocol (Invitrogen). Stat3 (79D7), NF-κB p65, and β-actin (13E5) rabbit mAbs (Cell Signaling Technology, Danvers, MA) were used for detection. Western blots were analyzed by densitometric scanning of immunoblots by the Biorad VersaDoc imaging system (Bio-Rad, Hercules, CA).

Transfection of STAT3 decoy and mismatched oligodeoxyribonucleotides

Phosphorothioated ODNs used for STAT3 decoys were purchased from Sigma-Genosys Biotechnologies (The Woodlands, TX). The decoy sequences, 5′-GATCC*TTCTGGGAATT*CCTAGATC-3′ and 3′-CTAGG*AAGACCCTTAA*GGATCTAG-5′ for the Stat3 decoy and 5′-GATCC*TTCTGGGCCGT*CCTAGATC-3′ and 3′-CTAGG*AAGACCC GGCA*GGATCTAG-5′ for the mismatched STAT3 decoy, were used in published studies (Xu *et al.*, 2003). Single-stranded ODNs were annealed by incubation at 65 °C for 10 minutes and then cooled to room temperature for 2 hours. Double-stranded decoys were transfected into monocytes 24 hours before stimulation at a final concentration of 2 μM by using Superfect (Qiagen, Valencia, CA) following the manufacturer's instruction.

Treatment with sense/scrambled and antisense oligodeoxyribonucleotides for SOCS3

The antisense ODN sequences for SOCS3 were selected from published literature (Lovibond *et al.*, 2003). Control ODNs for SOCS3 consisted of complementary sense ODNs. All ODNs were end modified (three bases of 5′ and 3′ ends phosphorothioated) to limit DNA degradation, and all were HPLC-purified pre-use (Invitrogen). Macrophages (5×10^6 cells per well) were plated in six-well culture plates overnight. Cells were then transfected with SOCS3 sense and antisense ODNs at 2 μM concentration using Mirus TransIt-Oligo Transfection Reagent (Mirus Bio, Madison, WI) according to the manufacturer's protocols, and the incubation was continued for 24 hours. For the transfection control, monocytes were incubated with the transfection reagent alone.

Antibodies and reagents

A total of 1,400 W (Sigma, St Louis, MO) was given at a 10 $\mu g\,g^{-1}$ dose. STAT3 cell-permeable peptide and inactive control (EMD Chemicals, Billerica, MA) were used at 5 μM final concentrations. Rosi (Alexis Biochemical, Farmingdale, NY) was used at a 5 μM final concentration for *in vitro* experiments, and at 0.2 mg per mouse for i.p. injections. ELISAs for soluble TNF-α receptor were performed according to the manufacturer's specifications (R&D Systems, Minneapolis, MN). Phospho-Stat3 (Tyr705) (D3A7) rabbit mAb were obtained from Cell Signaling (Beverly, MA) and PPAR-γ (E-8) sc-7273 from Santa Cruz (Dallas, TX).

Cloning, expression, and purification of mIL-6 analogs and vaccine production

IL-6 analog vaccine was developed as previously described (Galle *et al.*, 2007). Briefly, wt mIL-6 were expressed in *E. coli* and purified by Ni-NTA affinity chromatography (Qiagen Nordic, Sverige, Denmark). Purity was assured by SDS-PAGEs. The analogs were adsorbed to $Al(OH)_3$ (Alhydrogel 1.3% Brenntag Biosector AIS, Frederikssund, Denmark) in accordance with the manufacturer's instructions. After $Al(OH)_3$ adsorption, the mixture was washed three times in 0.9% (w/v) NaCl and finally suspended in 0.9% NaCl at a concentration of 39 μg per 100 μl suspension. The vaccines were stored at 4 °C.

Vaccine protocol

Mice were vaccinated subcutaneously on the dorsal side. Vaccinations were performed on days 0, 21, 42, and 63. Levels of plasma aAB-IL-6 were assessed by radio-immunoassay 14 days after each vaccination (Galle *et al.*, 2007). Blood samples were collected from the tail vein.

Statistical analysis

Data presented as means + SE. *P* values were calculated using a two-tailed Student's *t*-test for two samples of unequal variance. Statistical significance is indicated by an asterisk, and *P* values reported in figure legends.

CONFLICT OF INTEREST

The authors state no conflict to interest.

ACKNOWLEDGMENTS

This work was supported by grants from US National Institutes of Health and the Dermatology Foundation. We thank Kord Honda for dermatopathology consultations, Nicole Ward, Jennifer Ohtola, Denise Hatala, Candace Matheny, and Doina Draconeau for technical help, and John McGrath, George Stark, and Mansun Sy for critical comments. This study has also been supported in part by National Institutes of Health grant 5P30AR039750 via the Skin Diseases Research Center (SDRC—Morphology Core A) and the Ohio Department of Development—Center for Innovative Immunosuppressive Therapeutics (TECH 09-023).

SUPPLEMENTARY MATERIAL

Supplementary material is linked to the online version of the paper at http://www.nature.com/jid

REFERENCES

Akiyama H, Barger S, Barnum S *et al.* (2000) Inflammation and Alzheimer's disease. *Neurobiol Aging* 21:383–421

Awazawa M, Ueki K, Inabe K *et al.* (2011) Adiponectin enhances insulin sensitivity by increasing hepatic IRS-2 expression via a macrophage-derived IL-6-dependent pathway. *Cell Metab* 13:401–12

Baadsgaard O, Wulf HC, Wantzin GL *et al.* (1987) UVB and UVC, but not UVA, potently induce the appearance of T6- DR+ antigen-presenting cells in human epidermis. *J Invest Dermatol* 89:113–8

Campanholle G, Landgraf RG, Goncalves GM *et al.* (2010) Lung inflammation is induced by renal ischemia and reperfusion injury as part of the systemic inflammatory syndrome. *Inflamm Res* 59:861–9

Chatterjee PK (2010) Hepatic inflammation and insulin resistance in pre-diabetes - further evidence for the beneficial actions of PPAR-gamma agonists and a role for SOCS-3 modulation. *Br J Pharmacol* 160: 1889–91

Chomarat P, Banchereau J, Davoust J *et al.* (2000) IL-6 switches the differentiation of monocytes from dendritic cells to macrophages. *Nat Immunol* 1:510–4

Ciapponi L, Maione D, Scoumanne A *et al.* (1997) Induction of interleukin-6 (IL-6) autoantibodies through vaccination with an engineered IL-6 receptor antagonist. *Nat Biotechnol* 15:997–1001

Curran RD, Billiar TR, Stuehr DJ *et al.* (1989) Hepatocytes produce nitrogen oxides from L-arginine in response to inflammatory products of Kupffer cells. *J Exp Med* 170:1769–74

Cuzzocrea S, Pisano B, Dugo L *et al.* (2004) Rosiglitazone, a ligand of the peroxisome proliferator-activated receptor-gamma, reduces acute inflammation. *Eur J Pharmacol* 483:79–93

Faveeuw C, Fougeray S, Angeli V *et al.* (2000) Peroxisome proliferator-activated receptor gamma activators inhibit interleukin-12 production in murine dendritic cells. *FEBS Lett* 486:261–6

Feinstein DL, Spagnolo A, Akar C *et al.* (2005) Receptor-independent actions of PPAR thiazolidinedione agonists: is mitochondrial function the key? *Biochem Pharmacol* 70:177–88

Fosgerau K, Galle P, Hansen T *et al.* (2010) Interleukin-6 autoantibodies are involved in the pathogenesis of a subset of type 2 diabetes. *J Endocrinol* 204:265–73

Fujiwara N, Kobayashi K (2005) Macrophages in inflammation. *Curr Drug Targets Inflamm Allergy* 4:281–6

Galle P, Jensen L, Andersson C *et al.* (2007) Vaccination with IL-6 analogues induces autoantibodies to IL-6 and influences experimentally induced inflammation. *Int Immunopharmacol* 7:1704–13

Galle P, Svenson M, Bendtzen K *et al.* (2004) High levels of neutralizing IL-6 autoantibodies in 0.1% of apparently healthy blood donors. *Eur J Immunol* 34:3267–75

Gregorio J, Meller S, Conrad C *et al.* (2010) Plasmacytoid dendritic cells sense skin injury and promote wound healing through type I interferons. *J Exp Med* 207:2921–30

Hammad H, de Heer HJ, Soullie T *et al.* (2004) Activation of peroxisome proliferator-activated receptor-gamma in dendritic cells inhibits the development of eosinophilic airway inflammation in a mouse model of asthma. *Am J Pathol* 164:263–71

Hammerberg C, Duraiswamy N, Cooper KD (1996) Reversal of immunosuppression inducible through ultraviolet-exposed skin by in vivo anti-CD11b treatment. *J Immunol* 157:5254–61

Hansen MB, Svenson M, Diamant M *et al.* (1991) Anti-interleukin-6 antibodies in normal human serum. *Scand J Immunol* 33:777–81

Hansson GK (2005) Inflammation, atherosclerosis, and coronary artery disease. *N Engl J Med* 352:1685–95

Harbrecht BG, Nweze I, Smith JW *et al.* (2012) Insulin inhibits hepatocyte iNOS expression induced by cytokines by an Akt-dependent mechanism. *Am J Physiol Gastrointest Liver Physiol* 302:G116–22

Hasegawa-Moriyama M, Ohnou T, Godai K *et al.* (2012) Peroxisome proliferator-activated receptor-gamma agonist rosiglitazone attenuates postincisional pain by regulating macrophage polarization. *Biochem Biophys Res Commun* 426:76–82

Hotchkiss RS, Nicholson DW (2006) Apoptosis and caspases regulate death and inflammation in sepsis. *Nat Rev Immunol* 6:813–22

Jiang C, Ting AT, Seed B (1998) PPAR-gamma agonists inhibit production of monocyte inflammatory cytokines. *Nature* 391:82–6

Lawrence T (2009) The nuclear factor NF-kappaB pathway in inflammation. *Cold Spring Harb Perspect Biol* 1:a001651

Li Y, de Haar C, Peppelenbosch MP *et al.* (2012) SOCS3 in immune regulation of inflammatory bowel disease and inflammatory bowel disease-related cancer. *Cytokine Growth Factor Rev* 23:127–38

Liu H, Wang S, Sun A *et al.* (2012) Danhong inhibits oxidized low-density lipoprotein-induced immune maturation of dentritic cells via a peroxisome proliferator activated receptor gamma-mediated pathway. *J Pharmacol Sci* 119:1–9

Lovibond AC, Haque SJ, Chambers TJ *et al.* (2003) TGF-beta-induced SOCS3 expression augments TNF-alpha-induced osteoclast formation. *Biochem Biophys Res Commun* 309:762–7

Lowry JL, Brovkovych V, Zhang Y *et al.* (2013) Endothelial nitric-oxide synthase activation generates an inducible nitric-oxide synthase-like output of nitric oxide in inflamed endothelium. *J Biol Chem* 288: 4174–93

Mao K, Chen S, Chen M *et al.* (2013) Nitric oxide suppresses NLRP3 inflammasome activation and protects against LPS-induced septic shock. *Cell Res* 23:201–12

Marinescu VD, Kohane IS, Riva A (2005) The MAPPER database: a multi-genome catalog of putative transcription factor binding sites. *Nucleic Acids Res* 33:D91–7

Meunier L, Bata-Csorgo Z, Cooper KD (1995) In human dermis, ultraviolet radiation induces expansion of a CD36+ CD11b+ CD1- macrophage subset by infiltration and proliferation; CD1+ Langerhans-like dendritic antigen-presenting cells are concomitantly depleted. *J Invest Dermatol* 105:782–8

Nagy L, Tontonoz P, Alvarez JG *et al.* (1998) Oxidized LDL regulates macrophage gene expression through ligand activation of PPARgamma. *Cell* 93:229–40

Odegaard JI, Ricardo-Gonzalez RR, Goforth MH *et al.* (2007) Macrophage-specific PPARgamma controls alternative activation and improves insulin resistance. *Nature* 447:1116–20

Pahan K, Sheikh FG, Liu X *et al.* (2001) Induction of nitric-oxide synthase and activation of NF-kappaB by interleukin-12 p40 in microglial cells. *J Biol Chem* 276:7899–905

Park EJ, Park SY, Joe EH *et al.* (2003) 15d-PGJ2 and rosiglitazone suppress Janus kinase-STAT inflammatory signaling through induction of suppressor of cytokine signaling 1 (SOCS1) and SOCS3 in glia. *J Biol Chem* 278:14747–52

Pearson TA, Mensah GA, Alexander RW *et al.* (2003) Markers of inflammation and cardiovascular disease: application to clinical and public health practice: A statement for healthcare professionals from the Centers for Disease Control and Prevention and the American Heart Association. *Circulation* 107:499–511

Puel A, Picard C, Lorrot M *et al.* (2008) Recurrent staphylococcal cellulitis and subcutaneous abscesses in a child with autoantibodies against IL-6. *J Immunol* 180:647–54

Qi F, Adair A, Ferenbach D *et al.* (2008) Depletion of cells of monocyte lineage prevents loss of renal microvasculature in murine kidney transplantation. *Transplantation* 86:1267–74

Qin H, Yeh WI, De Sarno P *et al.* (2012) Signal transducer and activator of transcription-3/suppressor of cytokine signaling-3 (STAT3/SOCS3) axis in myeloid cells regulates neuroinflammation. *Proc Natl Acad Sci USA* 109:5004–9

Ricote M, Li AC, Willson TM *et al.* (1998) The peroxisome proliferator-activated receptor-gamma is a negative regulator of macrophage activation. *Nature* 391:79–82

Rosen CJ (2007) The rosiglitazone story–lessons from an FDA Advisory Committee meeting. *N Engl J Med* 357:844–6

Sener G, Sehirli AO, Gedik N *et al.* (2007) Rosiglitazone, a PPAR-gamma ligand, protects against burn-induced oxidative injury of remote organs. *Burns* 33:587–93

Sikora JP, Chlebna-Sokol D, Andrzejewska E *et al.* (2008) Clinical evaluation of proinflammatory cytokine inhibitors (sTNFR I, sTNFR II, IL-1 ra), anti-inflammatory cytokines (IL-10, IL-13) and activation of neutrophils after burn-induced inflammation. *Scand J Immunol* 68:145–52

Sikora JP, Kuzanski W, Andrzejewska E (2009) Soluble cytokine receptors sTNFR I and sTNFR II, receptor antagonist IL-1ra, and anti-inflammatory cytokines IL-10 and IL-13 in the pathogenesis of systemic inflammatory response syndrome in the course of burns in children. *Med Sci Monit* 15:CR26–31

Takemura H, Suzuki H, Yoshizaki K *et al.* (1992) Anti-interleukin-6 autoantibodies in rheumatic diseases. Increased frequency in the sera of patients with systemic sclerosis. *Arthritis Rheum* 35:940–3

Tanaka T, Kishimoto T (2012) Targeting interleukin-6: all the way to treat autoimmune and inflammatory diseases. *Int J Biol Sci* 8:1227–36

Tilg H, Trehu E, Atkins MB *et al.* (1994) Interleukin-6 (IL-6) as an anti-inflammatory cytokine: induction of circulating IL-1 receptor antagonist and soluble tumor necrosis factor receptor p55. *Blood* 83: 113–8

Tsukahara Y, Morisaki T, Kojima M *et al.* (2001) iNOS expression by activated neutrophils from patients with sepsis. *ANZ J Surg* 71:15–20

Tsukamoto H, Hishinuma T, Suzuki N *et al.* (2004) Thiazolidinediones increase arachidonic acid release and subsequent prostanoid production in a peroxisome proliferator-activated receptor gamma-independent manner. *Prostaglandins Other Lipid Mediat* 73:191–213

Wheeler JL, Martin KC, Lawrence BP (2013) Novel cellular targets of AhR underlie alterations in neutrophilic inflammation and inducible nitric oxide synthase expression during influenza virus infection. *J Immunol* 190:659–68

Xing Z, Gauldie J, Cox G *et al.* (1998) IL-6 is an antiinflammatory cytokine required for controlling local or systemic acute inflammatory responses. *J Clin Invest* 101:311–20

Xu B, Bhattacharjee A, Roy B *et al.* (2003) Interleukin-13 induction of 15-lipoxygenase gene expression requires p38 mitogen-activated protein kinase-mediated serine 727 phosphorylation of Stat1 and Stat3. *Mol Cell Biol* 23:3918–28

Yu Z, Kone BC (2004) The STAT3 DNA-binding domain mediates interaction with NF-kappaB p65 and iuducible nitric oxide synthase transrepression in mesangial cells. *J Am Soc Nephrol* 15:585–91

Yu Z, Zhang W, Kone BC (2002) Signal transducers and activators of transcription 3 (STAT3) inhibits transcription of the inducible nitric oxide synthase gene by interacting with nuclear factor kappaB. *Biochem J* 367:97–105